A novel projection based electro-stereolithography (PES) process for production of 3D polymer-particle composite objects

Yayue Pan and Abhishek Patil
Department of Mechanical and Industrial Engineering, University of Illinois at Chicago, Chicago, Illinois, USA
Ping Guo
Department of Mechanical and Automation Engineering, Chinese University of Hong Kong, Hong Kong, and
Chi Zhou
Department of Industrial and Systems Engineering, University at Buffalo, Buffalo, New York, USA

Abstract

Purpose – Polymer-particle composites, which have demonstrated wide applications ranging from energy harvesting and storage, biomedical applications, electronics and environmental sensing to aerospace applications, have been investigated for decades. However, fabricating polymer-particle composites with controlled distribution of particles in polymer continues to be a fundamental challenge. As to date, a few additive manufacturing (AM) technologies can fabricate composites, however, with a limited choice of materials or limited dispersion control. Against this background, this research investigated a hybrid polymer-particle composite manufacturing process, projection electro-stereolithography (PES) process, which integrates electrostatic deposition and projection based stereolithography (SL) technologies.

Design/methodology/approach – In PES process, a photoconductive film collects charged particles in the regions illuminated by light. Then, collected particles are transferred from the film to a polymer layer with defined patterns. Lastly, a digital mask is used to pattern the light irradiation of the digital micromirror device chip, selectively curing the photopolymer liquid resin and particles of that layer. By transferring particles from the photoconductive film to the photopolymer in a projection-based SL system, multi-material composites with locally controlled dispersions could be produced. A proof-of-concept PES testbed was developed. Various test cases have been performed to verify the feasibility and effectiveness of the developed approach.

Findings – Challenges in this novel AM process, including process design, particle patterning and transferring, are addressed in this paper. It is found that particles can be transferred to a layer of partially cured resin completely and accurately, by using the stamping approach. The transferring rate is related to stamping force and degree of conversion of the recipient layer. The developed hybrid process can fabricate polymer-particle composites with arbitrary dispersion pattern, unlimited printable height and complicated geometries.

Originality/value – Although an electrostatic deposition process has been investigated as a 3D printing technology for many years, it is the first attempt to integrate it with projection SL for fabricating multi-material polymer composite components. The novel hybrid process offers unique benefits including local dispersion control, arbitrary filling patterns, wide range of materials, unlimited printable height and arbitrary complicated geometries.

Keywords Stereolithography, Electrophoretic deposition, Multi-material printing, Polymer-particle composite

Paper type Research paper

1. Introduction

Additive manufacturing (AM) of multi-material composites has attracted considerable research interest. For example, commercial machines like the Objet Connex 3D printer from Stratasys and ProJet 5500 from 3D systems have recently entered into the market with the capability of printing multiple photopolymers in one build. Both of them use the multi-jet printing process, which has unique advantage in combining materials and scalability. Yet, it only accepts liquid photopolymers, and the selection of materials is constrained by their flow ability in the inkjet print head. In addition to jetting technique, some other AM techniques have also been investigated, such as multi-nozzle deposition (Khalil *et al.*, 2005), multi-vat photopolymerization (Zhou *et al.*, 2011), selective laser sintering of multi-metallic materials (Liew *et al.*, 2001, 2002; Jackson *et al.*, 2000) etc. Those research attempts made it feasible to fabricate 3D multi-polymer or multi-metal composite parts using AM principles. In contrast, few techniques have been developed for fabricating polymer-particle composites. Current AM techniques for polymer-particle composites are usually based on solidifying a suspension of metallic/polymer-particles and liquid, which is usually prepared by blending and hence has little control on

The current issue and full text archive of this journal is available on Emerald Insight at: **www.emeraldinsight.com/1355-2546.htm**

Rapid Prototyping Journal
23/2 (2017) 236–245

[DOI 10.1108/RPJ-02-2016-0030]

Received 24 February 2016
Accepted 4 May 2016

local dispersion (Bartolo and Gaspar, 2008; Kumar and Kruth, 2010; Wurm *et al.*, 2004).

Polymer-particle composites have shown wide applications, ranging from energy harvesting and storage, biomedical applications, electronics and environmental sensing to aerospace applications (Shahinpoor *et al.*, 1998, 2007; Sahinpoor, 2003; Shahinpoor and Kim, 2005). However, fabricating polymer-particle composites with controlled distribution of particles in a host polymer material continues to be a fundamental challenge (Srivastava *et al.*, 2014). To address such a significant challenge, this paper explores the feasibility of developing a hybrid AM process by integrating electrostatic deposition with stereolithography (SL) process.

Electrostatic deposition has been investigated and successfully developed as a 3D printing technique by researchers including Kumar Group at University of Florida, Cormier Groups at North Carolina State University and Rochester Institute of Technology (Jones *et al.*, 2010; Kumar *et al.*, 2003, 2004; Kumar and Dutta, 2003, 2004; Cross, 1987; Das, 2004; Cormier *et al.*, 2000; Arciniegas, 2013). The capability of depositing multiple particles (polymers, metals, etc.) has been shown in these pioneer works. 3D objects have been successfully printed using both metal particles like iron powders and polymer particles like nylon powders. Challenges have also been identified, including particle transfer mechanisms, distortions occurred during fusing and compaction, surface defects due to residual charges and limited printable height.

Unlike these pioneer studies on electrostatic deposition-based 3D printing, this study aims on fabrication of polymer-particle composite parts, instead of single-material parts. Additionally, this study explores a hybrid process that integrates electrostatic deposition with the SL process. In the hybrid process, electrostatic deposition is used only for 2D patterning of particle deposition, whereas the 3D structure is achieved by the SL approach. Therefore, advantages of electrostatic deposition in depositing metal/polymer/ceramic particles with programmed patterns are fully used, while challenges identified in others' work, such as surface defects and limited printable height, are avoided in the proposed process. Section 2 describes the entire process, hardware and software in detail. Section 3 discusses particle deposition and transfer in the PES process, followed by Section 4 in which test cases are presented and experimental results are analyzed. Conclusions and future work are presented in Section 5.

2. Process description

2.1 Overview of PES process

Projection SL technology offers high material resolution, dimensional accuracy and good surface quality. By using a DLP projector and liquid photo-curable resin, we can define and control the pattern of the images that will be projected on a surface area and, in turn, control the shape of the cured layer. Alternatively, electrostatic deposition digital printing, also known as electrophotographic printing, has achieved a high level of productivity and maturity in mainstream 2D printing, and the feasibility of 3D printing has been shown (Jones *et al.*, 2010). However, the majority of the pioneer work has been done by incorporating electrophotography into a powder-bed fusion system, which suffers from limited build height problems and fusing distortions (Jones *et al.*, 2010; Kumar *et al.*, 2003, 2004; Kumar and Dutta, 2003).

In this study, the proposed projection electro-stereolithography (PES) process consists of three parts:

1 electrostatic deposition of particles with a certain pattern;
2 transferring of particles to photopolymer; and
3 photo-curing of polymer-particle composites.

Specifically, a photo-curable resin and metal/polymer particles are used as the feedstock. Digital masks are used in both the particle deposition part and photo-curing part. The proposed PES approach opens up new ways of controlling material distributions and processing by incorporating the electrostatic deposition mechanism into an SL-based AM process. Specifically, the configuration of PES system is shown in Figure 1, and the process follows seven main steps:

1 *Initialization*: The 3D digital model is loaded in the process control software, and sliced into two sets of 2D images: one for liquid resin photo-curing (image set L) and the other for particle patterning (image set P). The platform and the particle-collecting plate are homed. The projection and the electrostatic deposition units are initialized.

Figure 1 Illustration of PES process

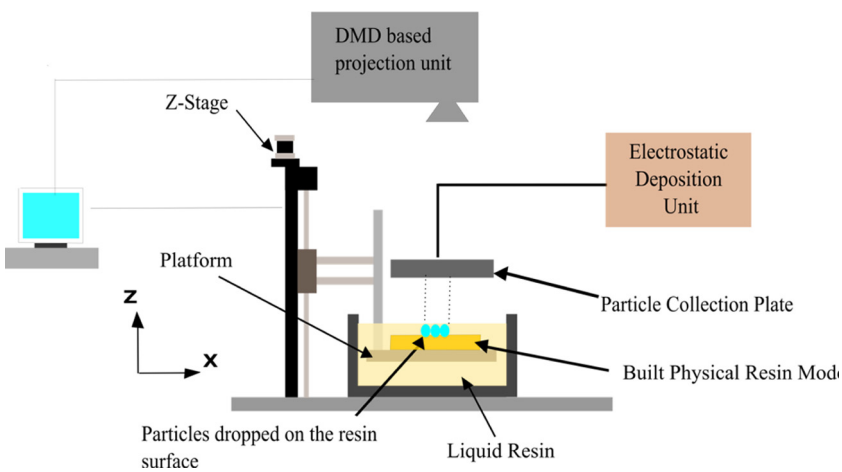

2 *Curing*: The resin-curing image of that layer in the image set L (photo-curing set) is projected to the photopolymer, to selectively cure the resin of that layer.
3 *Charging*: In the electrostatic deposition unit, the photoconductor surface is negatively sensitized with electrostatic charging by means of a corona-charging device or charging roller for the toner cartridge.
4 *Exposing*: In the electrostatic deposition unit, the photoconductor surface is scanned by the laser beam, which discharges the photoconductor and forms a latent image according to the particle deposition image of that layer (from image set P).
5 *Particle collecting*: In the electrostatic deposition unit, the developed image is then transferred to the particle collection plate. The charging roller positively charges the plate and the electrostatic force attracts the toner powder to jump on to the plate.
6 *Particle transferring*: The charged particle-collection plate is then moved to the surface of liquid resin by using two linear stages. Particles are then transferred to the photopolymer via the stamping transfer method (which is discussed in detail in Section 3.2).
7 *2nd-Curing*: The current layer of resin-curing image from image set L is projected again to fuse the newly transferred particles.

2.2 Experimental setup

A prototype machine has been developed, as shown in Figure 2(a). To reduce the prototype cost and simplify the system design, an off-the-shelf projector (Acer H6510BD) was modified and used as a DLP projection unit. Various projection settings including focus, keystone rectification, brightness and contrast have been adjusted to achieve a sharp projection image on the designed projection plane. The digital micromirror device (DMD) resolution in our system is 1,024 × 768, and the envelope size is set at 5.35 × 4.06 inches. Three precise linear motion stages from Oriental Motor USA Co. (Elk Grove Village, IL) are used to drive the platform and the particle-collecting plate. In the electrostatic deposition unit, a photoconductive film is used to collect charged particles on a plate in regions illuminated by light. The Z-stage elevator located under the DMD-based projection unit drives the build platform up and down. The other two linear stages, Z-stage and the X-stage, are used to collect particles from the electrostatic deposition unit and transfer them to the built model on the build platform. A high performance four-axes motion control board with 28 bi-directional I/O pins from Dynomotion Inc. (Calabasas, CA) is used to drive linear stages. The electrostatic deposition unit is built from parts of an HP LaserJet (P1102w) printer.

A mask image-planning testbed has been developed using the C++ language. It integrates the geometry slicing, digital mask generation, image loading, projection and motion controlling. Digital masks are constructed according to the material distribution of the sliced layer. Mask image projection is synchronized with the stage movement. The flow chart of the PES process and the graphical user interface (GUI) of the test bed is shown in Figure 2(b).

Figure 2 (a) A developed prototype machine; (b) flow chart and GUI of the developed software system

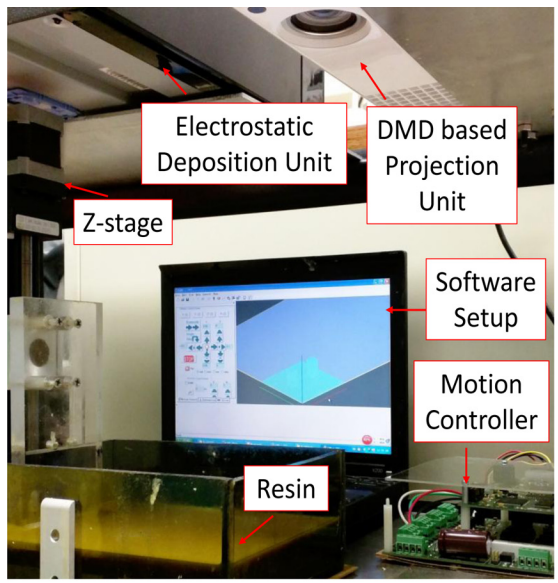

(a)

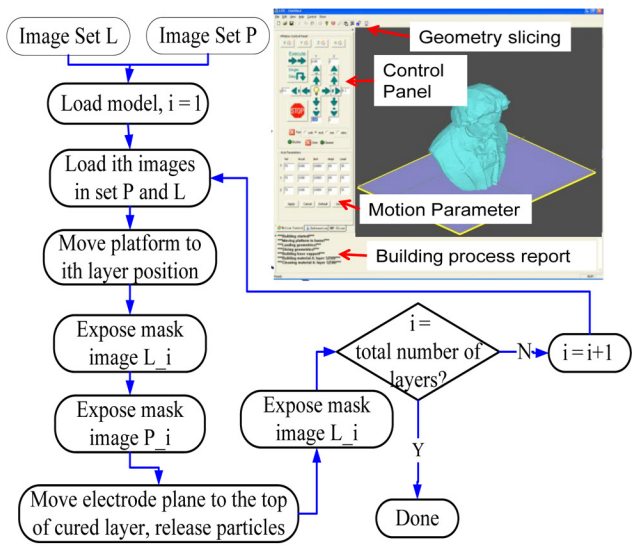

(b)

3. Physical modeling of material deposition

3.1 Collecting particles

Electrostatic digital printing, also known as electrophotography printing, is a well-established and commonly used process in 2D laser printers, where the toner is selectively deposited onto a piece of paper to produce the desired printed copy.

Figure 3 shows an illustration of a typical electrostatic deposition process. The photoconductive surface of the drum is charged by a corona discharge. This charged photoconductive surface is then exposed to a digital mask so that the charge on the surface is dissipated to the ground. Because of the electrostatic forces, the charged particles dropped from the image developer adhere to the surface when

Figure 3 (a) Schematic illustration of the electrophotographic printing; (b) force model for the toner–photoelectrode arrangement

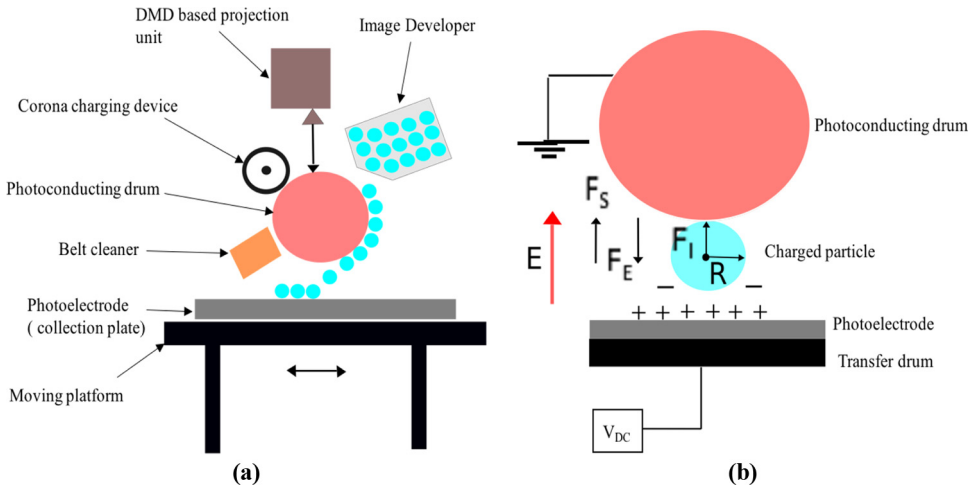

it is brought in vicinity of the latent image. This pattern is then transferred to the photo-electrode with the help of an electric field. Thus, the charged particles are collected on the photo-electrode surface. Lastly, the photoconductive surface is cleaned for next particle pattern deposition.

The relationship between electric field intensity and the potential applied to the build platform is computed using Gauss laws (Cross, 1987; Kumar and Dutta, 2004). According to the special conditions in PES process, a simplified model of electric field could be derived as:

$$E\left(\frac{p}{\sigma_S}\right) = \frac{V_{DC} + \frac{\rho_1 d_1^2}{2K_1 \in_0} - \frac{\rho_2 d_2^2}{2K_2 \in_0} + \frac{p}{\in_0}(\sigma_s + \rho_1 d_1)}{K_1\left(\frac{d_1}{K_1} + \frac{d_2}{K_2} + p\right)} \quad (1)$$

In the above equation, V_{DC} is the voltage applied across the build platform; p is the height of the printed part (or previously printed layers); d_1 is the thickness of the printed powder layer; d_2 is the thickness of the photoconductive layer; K_1, K_2 are the relative permittivity of the printed powder layer and the photoconductive drum layer, respectively; ρ_1, ρ_2 denote the charge per unit volume in the fresh printed layer and photoconductive drum layer, respectively; σ_s is the charge per unit area deposited on the print surface, and $\in_0$ is the permittivity of the air.

Now the electrostatic detachment force F_E exerted on a spherical particle having a radius R and charge q from the photoconductor by an applied field of magnitude E is given by (Rimai *et al.*, 1996, 2003):

$$F_E = \beta qE - 4\lambda\pi\varepsilon_0 R^2 E^2 \quad (2)$$

In an actual scenario, however, a particle is partially surrounded by air and partially in contact with the photoconductive surface. For these conditions, it is not possible to draw a Gaussian surface around the particle, so the part of the toner particle, which is closest to the photoconductor surface, will have the greatest effect on the electrostatic attraction (Rimai *et al.*, 2003). Hence, equation (2) would reduce to:

$$F_E = qE \quad (3)$$

Also the toner particles are held to the photoconductor surfaces by two forces. The first is an electrostatic force F_1 caused by the toner particle inducing image charge within the photoconductor and is given by:

$$F_I = -\beta\frac{q^2}{4\pi\varepsilon_0(2R)^2} \quad (4)$$

The second force is F_s, arising from the surface forces such as those because of van der Waals' attraction. This force is given by the Johnson–Kendall–Roberts (JKR) equation (Rimai *et al.*, 2003; Johnson *et al.*, 1971):

$$F_s = -\frac{3}{2}\omega_A \quad (5)$$

where ω_A is the thermodynamic work of adhesion, which is related to the surface free energies of the toner particle Υ_T and photoconductor Υ_S, as well as the interfacial energy by Υ_{TS}:

$$\omega_A = \Upsilon_T + \Upsilon_S + \Upsilon_{TS} \quad (6)$$

The approximate value of ω_A for a toner particle on an organic substrate is $\omega_A \sim 0.05\text{J/m}^2$ (Rimai and Quesnel, 2001). The force acting on the toner particle because of gravity F_W can be represented as:

$$F_W = mg = pVg \quad (7)$$

Therefore, the net force F_T acting on the particle to separate it from the photoconductive surface should be greater than zero for successful deposition of the particles on the collection plate. From equations (3)-(6), it could be written as:

$$\mathrm{F_T} = \mathrm{qE} + \rho\mathrm{VG} - [\mathrm{F_I} + \mathrm{F_S} + \mathrm{F_A}] > 0 \quad (8)$$

Here F_A is including all the adhesion and cohesion forces, other than van der Waals, double layer, chemical, hydrophobic forces (AL-Rubaiey, 2010).

3.2 Particle transfer mechanism

After collecting the particles with desired patterns successfully, particles are transferred from the collection film to cured resin surface using a stamping method, as illustrated in Figure 4. The yellow layer represents the current cured layer that needs to be filled with particles. The collection film is pressed on the layer surface with a certain stamping force F_s for approximately 2 s, and then peeled off from the surface with a velocity v_p. During the peeling-off process, there are a number of forces exerted on the particle, mainly an upward force F_E, downward force F_a and F_g, as denoted in Figure 5. F_E is the adhesion force from the collection film that prevents particles leaving from the film, mainly because of the electrostatic attraction. F_a is the adhesion force developed because of the cured layer that separates the particles from the film. F_a is a combined result of surface tension, viscous force, mechanical interlocking, etc., depending on the stamping force and layer surface conditions. F_g is the downward force due to gravity. When the total downward force is greater than the total upward force, a particle will be successfully transferred from the collection film to the resin layer surface.

Figure 5 analyzes forces applied on a particle during the transferring process, caused by particle–liquid interaction or particle–liquid–solid interaction in difference conditions. Because of the oxygen inhibition, the newly cured layer surface has a thin film of liquid resin. In addition, by controlling the curing time of the layer, the amount of liquid resin on the surface and degree of conversion of the resin could be tuned for more effective transferring. Besides, by applying sufficient stamping force and proper curing time, a particle–liquid–solid interaction can be formed to achieve complete and accurate transferring.

When the transfer process involves particle–liquid interaction only, as shown in Figure 5(a), the adhesion force F_a is mainly caused by the liquid bridge. Dynamics and rupture conditions of liquid bridges are widely studied (Benilov and Cummins, 2013; Gao *et al.*, 2011; Knospe and Haj-Hariri, 2012; Yang *et al.*, 2010; Bowden *et al.*, 2000; Nosonovsky and Bhushan, 2009; Chen *et al.*, 2014). The vertical component of liquid bridge force is typically modeled by analyzing the total free energy of the liquid bridge (Gao *et al.*, 2011):

$$F_a = \sigma \cdot l_t \cdot \sin(\theta_2 - \theta_1) + \Delta P \cdot A \quad (9)$$

where σ is the surface tension, ΔP is the difference between vapor pressure and liquid pressure, θ_1 is the contact angle, θ_2 is the deviation angle and l_t is the perimeter of the interfacial

Figure 4 Particle transfer process using stamping approach

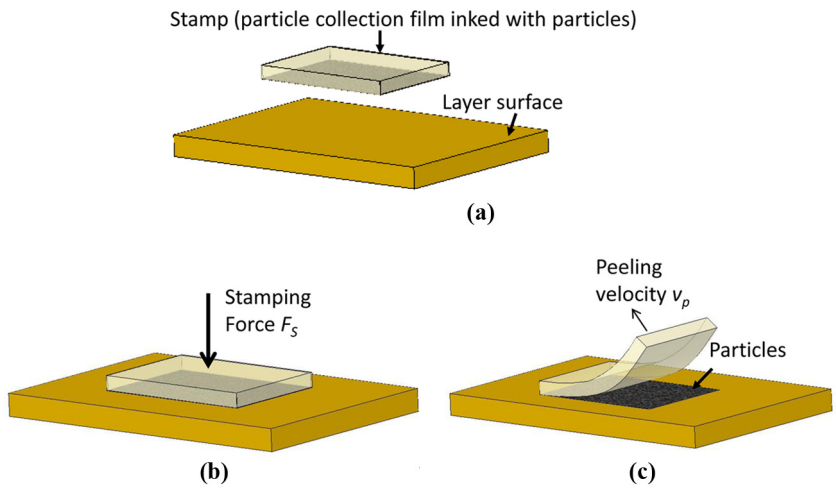

Notes: (a) Translate particle collection film to the desired position; (b) press particle collection film on the newly cured layer surface with a force F_s; (c) peel film off the surface with a velocity V_p

Figure 5 An illustration of the particle transfer process through elastomeric stamp

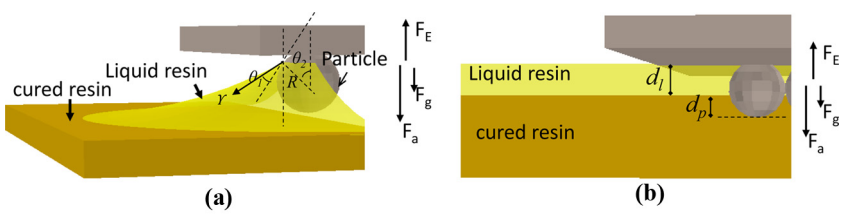

Notes: (a) Separation process with particle–liquid interaction; (b) separation process with particle–liquid–solid interaction

area A. Geometric relationships of these parameters are shown in Figure 5(a). The interfacial parameters could be approximated as:

$$l_t = \pi R \sin\theta_2 \tag{10}$$

$$A = \pi(R\sin\theta_2)^2 \tag{11}$$

$$\Delta P = \frac{2\sigma}{r_m} \tag{12}$$

where R is the radius of the particle, and r_m is the mean radii of the liquid interfacial profile. Substituting equations (10)-(12) into equation (9) leads to:

$$F_a = \sigma\pi R\sin\theta_2\left(\sin(\theta_2 - \theta_1) + \frac{2R\sin\theta_2}{r_m}\right) \tag{13}$$

It can be seen from equation (13) that, the transferring result depends on surface tension and contact angles greatly. With given liquid resin and particles, there is little room to adjust the adhesion force to improve transferring rate. Therefore, it is desired to press particles on the surface of partially cured resin layer and use the particle–solid interaction for transferring.

As shown in Figure 5(b), when the applied stamping force is sufficient, a particle–solid interaction will be formed. In such conditions, the adhesion force is much more complicated. Its modeling depends on many variables, such as the particle size, cured resin surface condition, liquid resin residue thickness and chemical properties of the particle and cured resin, etc. Process-related variables that influence the transferring results include stamping force F_s, stamping duration t, peeling velocity v_p and degree of conversion of the cured resin, which is determined by curing time T_c.

3.3 Transferring process characterization

Considering the modeling complexity, influences of curing time and the stamping force on the transfer rate were characterized experimentally. In this study, toner particles and an acrylic resin LS600M from EnvisonTEC Inc. were investigated. The stamping duration was fixed at 2 s, peeling velocity was fixed at approximately 5 mm/s, and a layer thickness of 152.3 μm was used.

In the experiments, particles were deposited on the collection film with a solid circle pattern and then transferred to a cured resin surface using the stamping approach. After stamping, the transferred rate was calculated by measuring the approximate surface area that was colored by the toner. For the LS600M resin and 152.3-μm layer thickness, a curing time of 15 s gives 100 per cent degree of conversion in our testbed.

To calibrate the influence of cured layer condition, particles' transferring tests were performed with a stamping force of 120 N on different cured resin surfaces that were fabricated by using curing time varied from 5 to 15 s. Three materials, namely, paper, Teflon film and polydimethylsiloxane (PDMS) film, were tested as the collection film substrate. It was found that when the collection film is either Teflon or PDMS, the particle pattern could be easily damaged during the transferring process. In contrast, the paper collection film gives a more reliable, stable and accurate transferring result. Measured transfer rates with paper collection film are plotted in Figure 6(a). It is clear that the transfer rate increases with the curing time; however, when the curing time reaches a critical point, the transfer rate decreases as the curing time increases. For the materials in our tests, a curing time of 9 s gives the best transferring performance.

Effects of stamping force on transferring rate were also calibrated experimentally. Transferring tests were also conducted by applying a stamping force varied from 27 to 158 N on resin surfaces that were cured by a curing time of 9 s. Transfer rates under varied stamping force are plotted in Figure 6(b). It is found that the transfer rate increases almost linearly with the stamping forces in the early range, i.e. from 27 to 110 N. After the transfer rate approaches a high value, i.e. 90 per cent, the increasing rate gets smaller.

4. Case study of heterogeneous composite printing

Three test cases have been performed to study the feasibility of the developed PES process for polymer-particle composite printing. The test particles used for this preliminary study were the toner particles of the HP LaserJet P1102w printer. The resin was the LS600M photopolymer from EnvisionTEC Inc. Different particle dispersion patterns were tested to evaluate the performance of the proposed process.

4.1 Stereolithography process test

First, to ensure that the proposed PES process and developed prototype systems have no issues in the printing 3D parts, two test cases were conducted. The manufacturing capability of SL of pure resin was verified by fabricating a gear and a cube array.

The first test case, gear model, constitutes 122 layers in total, including 3 base layers, with each layer thickness corresponding to 152.3 μm. Initial exposure time for the base

Figure 6 Effects of curing time and stamping force on particle transferring rate

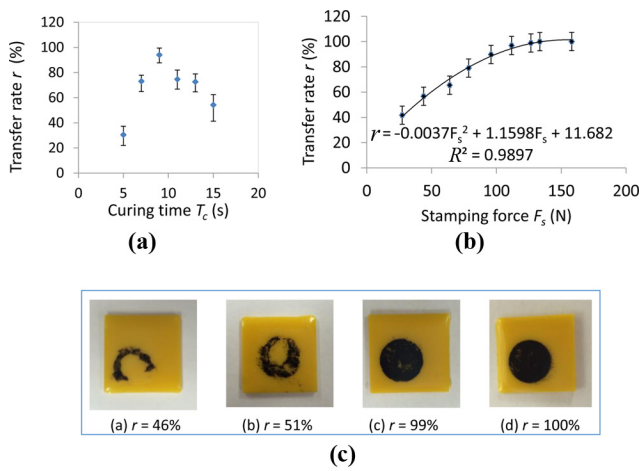

Notes: (a) Transfer rate vs curing time; (b) transfer rate vs stamping force; (c) test samples with varied transfer rates

layer is 150 s (2.5 min), whereas for the subsequent layer, it is 15 s each. A waiting time of 3 s is used when the stage goes down inside the resin tank to recover a uniform layer of fresh resin. Because a top-down projection has been adopted, after each layer, the platform travels down by a certain distance (approximately2.5 mm), and then, while retracting, it recoats one layer of liquid on the top. The gear design and fabricated part are shown in Figure 7(a) and (b).

The second test case for SL process validation is a cube array as shown in Figures 7(c) and (d). This model is sliced into 14 layers in total, 0 images in image set P and 14 images in image set L. A larger layer thickness of 203.2 μm is used for this test. The cube array, as shown in the Figure 7, is 38 × 38 mm.

These two simple tests show that the mask image-planning, light projection and liquid-curing components in the SL process worked properly and that the developed PES system is ready to receive particles for composite manufacturing.

4.2 Resin + particles photo-curing test

In this feasibility study, to eliminate the influence of unknown material properties on the PES process performance, the electrostatic unit of our testbed was developed from a modified off-the-shelf 2D laser printer, and we use the original toner cartridge particles to test the particle dropping and particle-resin curing processes in the developed PES system. However, it should be noted that any particles (metals, polymers) that can be electrostatically transferred could be used as the particle materials in the PES process.

4.2.1 Test of lateral distribution of particles with designed pattern

A cube array with particles forming letters "UIC" on its top left surface was tested to validate the capability of PES technology in selectively distributing particles on a lateral plane and programing spatial dispersion of particles in a host polymer. The process parameter setting as described in Section 3 was used.

Its computer-aided design (CAD) model and the fabricated part are shown in Figure 8. The model was sliced to 15 layers, generating 15 mask images in Image set L named "L_1, L_2 till L_15", and one mask image in Image set P named P_14. Image P_14 includes digital information of the "UIC" pattern for particle deposition and curing.

From Layer #1 to Layer #14, the part was built layer by layer using mask images in set L. After finishing the 14th layer, image P_14 was the input image for patterning particles. The laser scanned the photoconductive surface to form a latent image on the photoconductor surface. The toner particles were deposited on the particle collection plate by electrostatic force. Then, the stamping approach was used to transfer particles to the surface of the cured 14th layer.

After this, the image L_14 was exposed directly on the particles to improve the bonding between particles and cured resin surface. The exposure time was about 20 s. After the second curing step, the stage moved down to recoat a fresh resin layer for 15th layer curing.

To show the particles' distribution details, two parts were fabricated. Figure 8(b) shows the fabricated part without the 15th layer, which was fabricated by stopping the building process at the 14th layer. Figure 8(c) is the microscopic image of the red-circled area in Figure 8(c), showing particles on the 14th layer. From Figure 8(b) and (c), we can observe that the majority of particles have been transferred successfully from collection plate to resin surface. The "UIC" pattern formed by the electrostatic deposition process is retained pretty well after the transfer.

Another part is fabricated by completing the 15th layer. This way, the UIC patterned particles are covered by the top polymer layer. Figure 8(d) is the microscopic image of the same red-circled area of the model, which has a layer of cured resin covering the particles. Because the top layer resin is only 203-μm in thickness, the particles beneath are still visible, as shown in Figure 8(d).

Figure 7 (a) CAD model of spur gear; (b) fabricated gear; (c) CAD model of cube array; (d) fabricated cube array

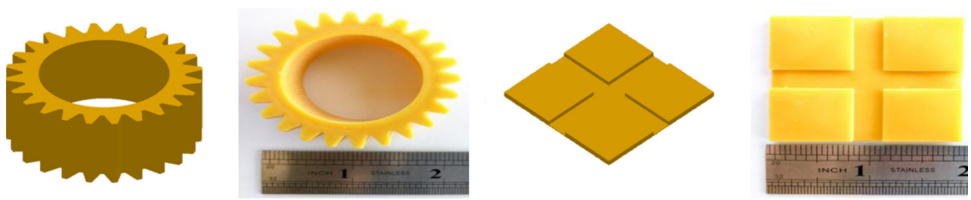

Figure 8 (a) CAD model; (b) fabricated cube array part without 15th layer; (c) microscopic images – top view of particles; (d) microscopic image – top view of particles after 15th layer

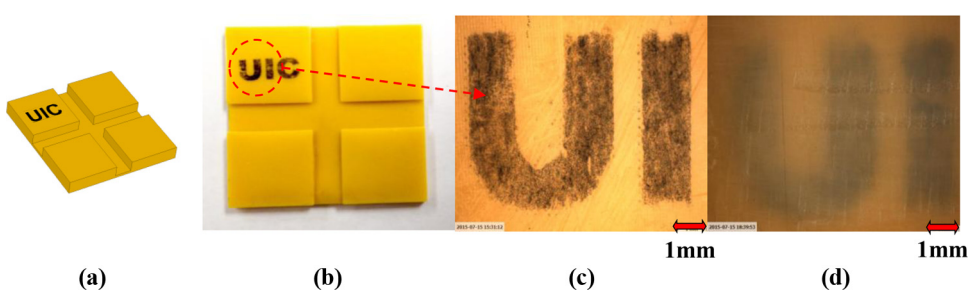

4.2.2 Test of vertical particle distribution control

A cuboidal model was used to test the capability of PES technology in selectively distributing particles in the vertical direction with designed patterns. Toner particles (black color) were imprinted on the 42nd and 46th layer of the 50 layers of the part. The process parameter setting as described in Section 3 was used.

The CAD model and a fabricated part are shown in Figures 9(a) and (b). The model is sliced to 50 layers. Image set L consists of 50 mask images named "L_1, L_2 till L_50", and image set P consists of two mask images named P_42 and P_46. These images deliver the digital information of the designed horizontal pattern for particle deposition and curing.

Figure 10(c) and (d) includes the microscopic images of the fabricated part. These figures show that particles are cured in designed layers. From the figures, the color distribution is very clear and even, such that we can distinctly differentiate between two particle layers from the part photo and microscopic images.

4.2.3 Test of horizontal particle distribution in the form of an electronic circuit

A circuit pattern was used to test the capability of the PES technology in selectively distributing particles in the horizontal plane with complicated patterns. The toner particles (black color) were imprinted on the 20th layer of the build part. The same manufacturing process with parameter settings as described in Section 3 was used.

The CAD model and the fabricated part are shown in Figure 10(a) and (b), respectively. The model was sliced to 20 layers. The image set L consists of 20 mask images named "L_1, L_2 to L_20", and the image set P consists of one mask image named P_21. These images deliver digital information of the designed horizontal pattern for particle deposition and curing.

Figure 10(c) and (d) includes the microscopic images of the part. Figure 10(c) shows the microscopic view of the electronic circuit pattern imprinted on the cured resin surface. It is clear that the particles are distributed with the designed circuit pattern. Figure 10(d) shows the microscopic image after another layer of resin was cured over the particle circuit pattern.

5. Conclusion and future work

A novel AM technology, PES, has been developed in this paper for polymer-particle composite printing. The proposed process uses electrostatic deposition approach to collect particles in a plate, and then uses stamping method to transfer particles to resin surface; hence, it is able to distribute particles into photopolymer layer by layer, with programmed patterns. Compared to existing multi-material 3D printing approach, which usually blends particles with liquid resin evenly first and then uses the paste as raw material, PES has a unique advantage in local control of particle dispersions, addressing the historical challenge in polymer-particle composite fabrication. This unique characteristic could open a new avenue for advanced composite materials design and AM functional products.

Feasibility and challenges in implementing this new technology are discussed in this paper. First, collection of one layer of particles each time avoids the historical research problems in extending 2D electrophotography technique into 3D printing. Second, transferring of particles with well-kept patterns has been investigated. Effects of collection plate materials, stamping force and curing time on transferring results are characterized. Accordingly, a proof-of-concept test

Figure 9 (a) CAD model; (b) top view of the fabricated model with toner particles in 42nd and 46th layer out of the 50 layers of the part; (c-d) microscopic image of two areas in the fabricated part

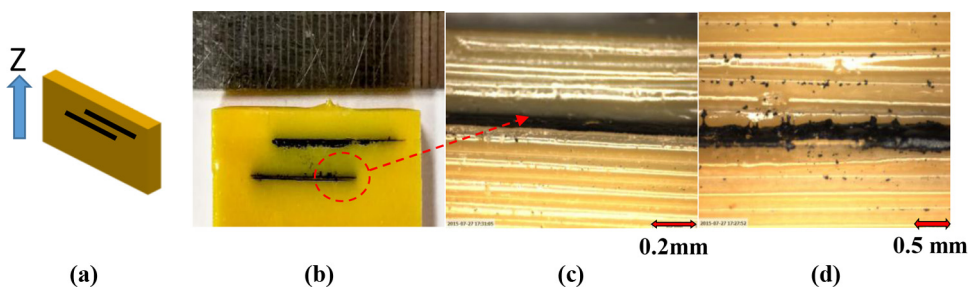

Figure 10 (a) CAD model; (b) top view of the fabricated model with toner particles on the 20th layer; (c) microscopic image – top view of the model of the transferred particles; (d) microscopic image – top view of the model after 21st resin layer is cured

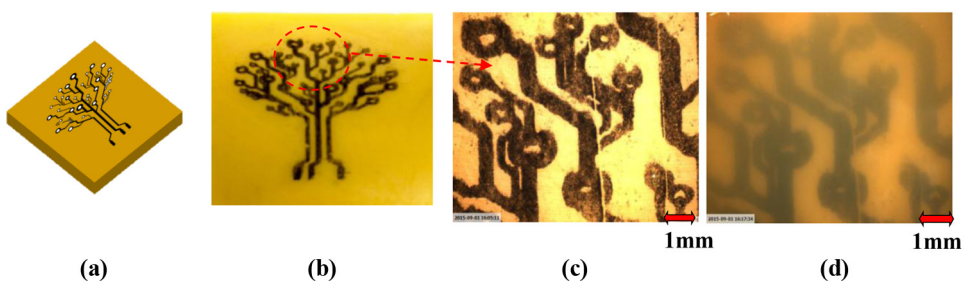

bed has been developed. Case studies verified the capability of this new process on building composites with programmable particle filling patterns.

As a novel manufacturing technology, considerable work remains to mature the process and the related prototype system to overcome potential challenges and improve its performance. Some on-going investigations in our group include:

- Testing other particles for electrostatic depositing and transferring.
- Investigating other approaches for improving the bonding between particles and cured resin, like thermal fusing.

References

AL-Rubaiey, H. (2010), "Toner transfer and fusing in electrophotography", *Graphic Arts in Finland*, Vol. 39 No. 1, pp. 1-28.

Arciniegas, R. (2013), "Towards the control of electrophotographic-based 3-dimensional printing: image-based sensing and modeling of surface defects", *Doctoral Dissertation*, Rochester Institute of Technology, Rochester, NY.

Bartolo, P.J. and Gaspar, J. (2008), "Metal filled resin for stereolithography metal part", *CIRP Annals – Manufacturing Technology*, Vol. 57 No. 1, pp. 235-238.

Benilov, E.S. and Cummins, C.P. (2013), "The stability of a static liquid column pulled out of an infinite pool", *Physics of Fluids*, Vol. 25 No. 11, 19 pages.

Bowden, N., Oliver, S.R.J. and Whitesides, G.M. (2000), "Mesoscale self-assembly: capillary bonds and negative menisci", *The Journal of Physical Chemistry B*, Vol. 104 No. 12, pp. 2714-2724.

Chen, H., Tang, T. and Amirfazli, A. (2014), "Liquid transfer mechanism between two surfaces and the role of contact angles", *Soft Matter*, Vol. 10 No. 15, p. 2503.

Cormier, D., Taylor, J., Unnanon, K., Kulkarni, P. and West, H. (2000), "Experiments in layered electro-photographic printing", *Proceedings of the SFF Symposium*, *Austin, TX*, pp. 267-274.

Cross, J. (1987), *Electrostatics: Principles, Problems and Applications*, IOP Publishing, Bristol.

Das, A.K. (2004), "An investigation on the printing of metal and polymer powders using electrophotographic solid freeform fabrication", *Doctoral Dissertation*, University of Florida, Gainesville, FL.

Gao, S., Jin, L., Du, J. and Liu, H. (2011), "The liquid-bridge with large gap in micro structural systems", *Journal of Modern Physics*, Vol. 2 No. 5, p. 404.

Jackson, B., Wood, K. and Beaman, J. (2000), "Discrete multi-material selective laser sintering (M 2 SLS): development for an application in complex sand casting core arrays", in *Proceedings of the Solid Freeform Fabrication Symposium*, *Austin, TX*, pp. 176-182.

Johnson, K., Kendall, K. and Roberts, A. (1971), "Surface energy and the contact of elastic solids", *Proceedings of the Royal Society of London A: Mathematical, Physical and Engineering Sciences*, *The Royal Society*.

Jones, J., Wimpenny, D., Gibbons, G. and Sutcliffe, C. (2010), "Additive manufacturing by electrophotography: challenges and successes", *NIP & Digital Fabrication Conference*, Society for Imaging Science and Technology, Austin, TX, Vol. 2010, pp. 549-553.

Khalil, S., Nam, J. and Sun, W. (2005), "Multi-nozzle deposition for construction of 3D biopolymer tissue scaffolds", *Rapid Prototyping Journal*, Vol. 11 No. 1, pp. 9-17.

Knospe, C.R. and Haj-Hariri, H. (2012), "Capillary force actuators: Modeling, dynamics, and equilibria", *Mechatronics*, Vol. 22 No. 3, pp. 251-256.

Kumar, A.V. and Dutta, A. (2003), "Investigation of an electrophotography based rapid prototyping technology", *Rapid Prototyping Journal*, Vol. 9 No. 2, pp. 95-103.

Kumar, A.V. and Dutta, A. (2004), "Electrophotographic layered manufacturing", *Journal of Manufacturing Science and Engineering*, Vol. 126 No. 3, p. 571.

Kumar, A.V., Dutta, A. and Fay, J.E. (2003), "Solid freeform fabrication by electrophotographic printing", 14th Solid Freeform Fabrication Symposium, Austin, TX.

Kumar, A.V., Dutta, A. and Fay, J.E. (2004), "Electrophotographic printing of part and binder powders", *Rapid Prototyping Journal*, Vol. 10 No. 1, pp. 7-13.

Kumar, S. and Kruth, J. (2010), "Composites by rapid prototyping technology", *Materials and Design*, Vol. 31 No. 2, pp. 850-856.

Liew, C.L., Leong, K.F., Chua, C.K. and Du, Z. (2001), "Dual material rapid prototyping techniques for the development of biomedical devices. Part 1: Space creation", *The International Journal of Advanced Manufacturing Technology*, Vol. 18 No. 10, pp. 717-723.

Liew, C.L., Leong, K.F., Chua, C.K. and Du, Z. (2002), "Dual material rapid prototyping techniques for the development of biomedical devices. Part 2: secondary powder deposition", *The International Journal of Advanced Manufacturing Technology*, Vol. 19 No. 9, pp. 679-687.

Nosonovsky, M. and Bhushan, B. (2009), "Multiscale effects and capillary interactions in functional biomimetic surfaces for energy conversion and green engineering", *Philosophical Transactions of the Royal Society A: Mathematical, Physical and Engineering Sciences*, Vol. 367 No. 1893, pp. 1511-1539.

Rimai, D. and Quesnel, D.J. (2001), *Fundamentals of Particle Adhesion*, Global Press, Srbija.

Rimai, D.S., Adhesion, S.o.P. and Society, A. (1996), "Advances in particle adhesion: selected papers", Symposium on Particle Adhesion at the 17th annual meeting of the Adhesion Society, Orlando, FL.

Rimai, D.S., Weiss, D.S. and Quesnel, D.J. (2003), "Particle adhesion and removal in electrophotography", *Journal of Adhesion Science and Technology*, Vol. 17 No. 7, pp. 917-942.

Shahinpoor, M. (2003), "Ionic polymer–conductor composites as biomimetic sensors, robotic actuators and artificial muscles – a review", *Electrochimica Acta*, Vol. 48 No. 14, pp. 2343-2353.

Shahinpoor, M. and Kim, K.J. (2005), "Ionic polymer–metal composites: IV: industrial and medical applications", *Smart Materials and Structures*, Vol. 14 No. 1, pp. 197-214.

Shahinpoor, M., Kim, K.J. and Mojarrad, M. (2007), *Artificial Muscles: Applications of Advanced Polymeric Nanocomposites*, CRC Press, Boca Raton, FL.

Shahinpoor, M., Bar-Cohen, Y., Simpson, J.O. and Smith, J. (1998), "Ionic polymer-metal composites (IPMCs) as biomimetic sensors, actuators and artificial muscles – a review", *Smart Materials and Structures*, Vol. 7 No. 6, pp. R15-R30.

Srivastava, S., Schaefer, J.L., Yang, Z., Tu, Z. and Archer, L.A. (2014), "25th anniversary article: polymer–particle composites: phase stability and applications in electrochemical energy storage", *Advanced Materials*, Vol. 26 No. 2, pp. 201-234.

Wurm, G., Tomancok, B., Holl, K. and Trenkler, J. (2004), "Prospective study on cranioplasty with individual carbon fiber reinforced polymere (CFRP) implants produced by means of stereolithography", *Surgical Neurology*, Vol. 62 No. 6, pp. 510-521.

Yang, L., Tu, Y. and Fang, H. (2010), "Modeling the rupture of a capillary liquid bridge between a sphere and plane", *Soft Matter*, Vol. 6 No. 24, p. 6178.

Zhou, C., Chen, Y., Yang, Z.G. and Khoshnevis, B. (2011), "Development of multi-material mask-image-projection-based stereolithography for the fabrication of digital materials", Annual Solid Freeform Fabrication Symposium, Austin, TX.

Further reading

Santosa, J., Jing, D. and Das, S. (2002), *Experimental and Numerical Study on the Flow of Fine Powders from Small-Scale Hoppers Applied to SLS Multi-Material Deposition – Part I*, Vol. 1001, Ann Arbor, MI, pp. 48109-52125.

Corresponding author

Yayue Pan can be contacted at: yayuepan@uic.edu